JOURNAL OF MATERIALS SCIENCE **34** (1999) 1809–1813

Synthesis of castable sodium zirconium phosphate monoliths employing reactions between zirconyl nitrate hydrate and condensed phosphates

B. T. LYNCH, P. W. BROWN, J. R. HELLMANN
Department of Materials Science and Engineering, Pennsylvania State University, USA

Reactions between zirconyl nitrate hydrate and condensed phosphates can be used to produce castable low CTE sodium zirconium phosphate (NZP) monoliths. Reaction between sodium nitrate, zirconyl nitrate hydrate and condensed phosphoric acid at room temperature (alkali nitrate method) produces monoliths having a heterogeneous microstructure, which are multiphasic in appearance. Except for the presence of crystalline sodium nitrate, they are X-ray amorphous. Differential thermal analysis revealed two distinct exothermic crystallization events when these materials are heated. The first event, with an onset temperature of 650 °C, is the result of NZP and ZrO_2 crystallization. The second is the result of ZrP_2O_7 crystallization. Reaction between zirconyl nitrate hydrate and condensed sodium phosphate (condensed alkali phosphate method) results in a more homogeneous microstructure in which crystalline zirconium hydrogen phosphate hydrate and sodium nitrate are present. Two exothermic peaks, with onset temperatures of approximately 570 and 860 °C, are observed. The first exotherm is the result of NZP, ZrO_2 and ZrP_2O_7 crystallization; the second exotherm is the result of a further NZP formation. After heating materials made by these two methods at 940 °C for 24 h, the condensed-alkali-phosphate-method-derived material converted to phase-pure NZP, while the alkali-nitrate-method-derived material contained ZrP_2O_7. The differences in phase evolution between the materials prepared by these two methods are attributable to the differences in chemical and microstructural homogeneity that result from the reactants used.

1. Introduction

Sodium zirconium phosphate (NZP), $NaZr_2P_3O_{12}$, and isostructural materials of varied compositions, were first studied in the late 1960s [1]. Technological interest in these materials grew as solid-state electrolytes for use in thermoelectric generators; materials of the general composition $Na_{1+x}Zr_2P_{3-x}Si_xO_{12}$ were synthesized [2], and it was determined that the composition $Na_3Zr_2PSi_2O_{12}$ behaves as a fast ion conductor [3]. In studying the coefficients of thermal expansion of compositions in this solid-solution series, it was found that for $x = 1$, a slight contraction takes place between room temperature and 500 °C [4]. At low silicon concentrations, the $Na_{1+x}Zr_2P_{3-x}Si_xO_{12}$ system was found to exhibit low thermal expansion behaviour [5]. As a result of this, observation on the low thermal expansion properties of these materials was stimulated. The low thermal expansion behaviour of these materials was found to be the result of a thermal expansion anisotropy, in which the coefficient of thermal expansion is positive in some crystallographic directions and negative in others. Further research focused on the silicon-free NZP end member, and the ability to tailor the thermal expansion of this material through chemical substitutions for the sodium and zirconium ions [6, 7]. Applications of interest include mirror substrates and instrument supports on space craft, lithography instruments, cookware and crucibles, as well as catalyst supports in automotive exhaust systems [8, 9].

NZP powders have been synthesized by a number of conventional methods, including solid-state reaction and sol-gel techniques. Fabrication of ceramic components requires consolidation of powders and sintering. Although densification of both solid-state and sol-gel NZP powders has been achieved, the strengths of these materials are generally low. The low strengths of materials exhibiting thermal expansion anisotropy have been attributed to microcracking. However, some applications for these materials, such as catalyst supports, filters and mirror substrates, which do not experience high mechanical loading in service, and a low density, near net-shape, castable, low thermal expansion monolith would be desirable.

The current study focuses on chemical processes for the synthesis of castable NZP monoliths. These techniques employ room temperature reactions between

zirconyl nitrate hydrate and viscous condensed phosphate solutions. These condensed phosphate solutions consist of phosphate chains of different lengths. The relative proportions of these phosphate chains are dependent upon the M_2O/P_2O_5 ratio, where $M = H^+$ in the case of a condensed phosphoric acid solution, called polyphosphoric acid; and M is a mixture of both H^+ and alkali ions in condensed alkali phosphate solutions. The procedures developed for synthesis of castable NZP monoliths are presented, and the phase evolution and microstructures observed in materials synthesized by these techniques are compared and discussed.

2. Experimental procedure

2.1. Synthesis of NZP monoliths

Two routes for the synthesis of castable NZP materials employing different reactants were investigated. They will be referred to as the *alkali nitrate method* and the *condensed alkali phosphate method*. The names are indicative of the source of the alkali ion.

1. *Alkali nitrate method*: stoichiometrically required amounts of −325 mesh $NaNO_3$ and $ZrO(NO_3)_2{\cdot}2H_2O$ were mixed with polyphosphoric acid. The reactants were mixed vigorously until a homogeneous mixture having a putty-like consistency was achieved. Samples were allowed to cure at room temperature without applied pressure.

2. *Condensed alkali phosphate method*: a 50 wt % P_2O_5 solution was made by adding deionized water to 85 wt % H_3PO_4. A 25 wt % $NaPO_3$ solution was made by adding deionized water to $NaH_2PO_4{\cdot}H_2O$. A sodium phosphate solution with a molar ratio of sodium to phosphate (Na : P) of 1 : 3 was made from these stock solutions. This phosphate solution was heated with stirring for 5 h on a hot-plate/stirrer set at 120 °C, resulting in a condensed sodium phosphate composed of approximately 20 wt % water. The stoichiometrically required amount of $ZrO(NO_3)_2{\cdot}H_2O$ was then added, and reactants were mixed together vigorously and were allowed to cure at room temperature without applied pressure.

2.2. Characterization

Phases were identified before and after heat treatment by powder X-ray diffraction. Imaging of fracture surfaces of samples was achieved by using both an environmental scanning electron microscope (SEM) and a conventional SEM. Differential thermal analysis (DTA) was performed to assess reaction sequences during heating at a rate of 40 °C min^{-1}.

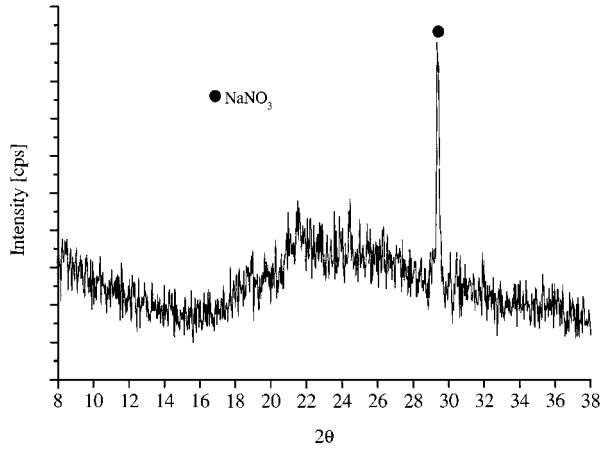

Figure 1 X-ray diffraction pattern of NZP precursor material prepared by the *alkali nitrate method* and cured at room temperature.

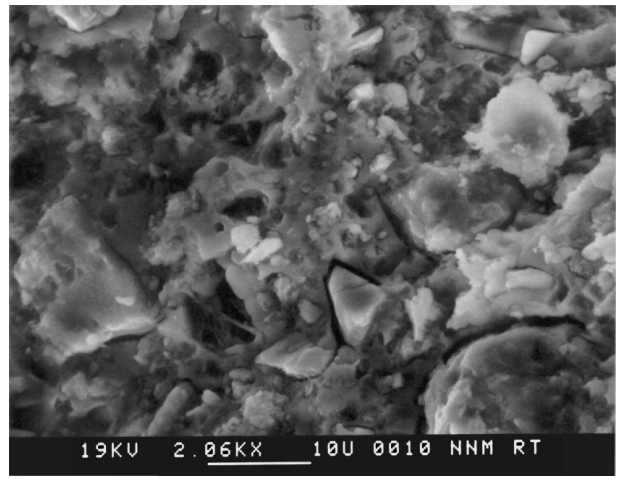

Figure 2 A micrograph of a low porosity region of NZP precursor material prepared by the *alkali nitrate method* and cured at room temperature.

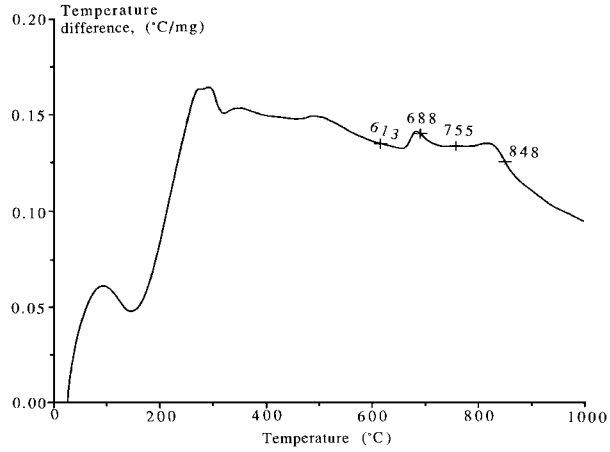

Figure 3 DTA curve obtained when NZP precursor material prepared by the *alkali nitrate method* is heated from 550 to 1050 °C.

3. Results and discussion

3.1. *Alkali nitrate method*

Fig. 1 is the X-ray diffraction pattern of a sample cured at room temperature. Crystalline sodium nitrate is present; however, the sample is largely X-ray amorphous, as indicated by the amorphous hump from approximately 17 to 30° 2θ. Fig. 2 is a micrograph of a fracture surface of a relatively dense region in this sample. The material is multiphasic and heterogeneous in appearance. This microstructure, as well as evidence of localized concentrations of sodium in samples, indicates that this synthesis technique does not produce the homogeneity that techniques, such as sol-gel synthesis, are capable of achieving.

Fig. 3 shows the DTA curve obtained when the alkali nitrate derived material was heated between 550

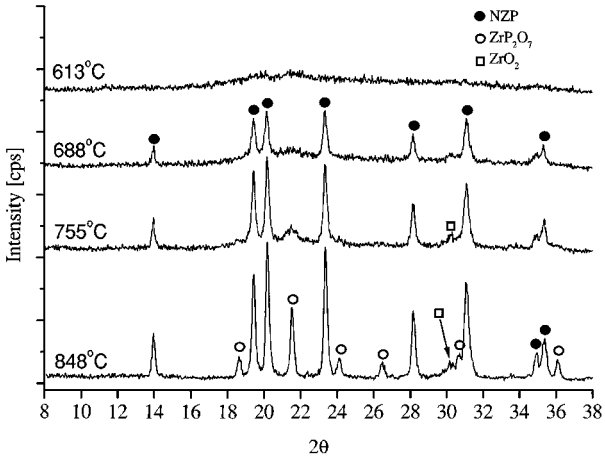

Figure 4 X-ray diffraction patterns obtained after precursor material prepared by the *alkali nitrate method* has been heated to 613, 685, 755 and 848 °C.

and 1050 °C. Two exothermic peaks are present. The first event has an onset temperature of approximately 650 °C, while the second event lacks a distinct onset temperature, as the two events appear to overlap. To determine the reaction mechanisms further, DTA runs were stopped at selected temperatures, the samples cooled, and X-ray diffraction analyses carried out to determine the crystalline phases present. These temperatures are indicated on Fig. 3. These patterns are shown in Fig. 4. The X-ray diffraction patterns obtained show the material is X-ray amorphous at 613 °C, a temperature below that of the onset of the first exotherm. At 685 °C, a temperature just above the peak of the first DTA exotherm, the most intense diffraction peak for ZrO_2 (30° 2θ) and NZP diffraction peaks are present, indicating that the first exotherm is the result of NZP and ZrO_2 crystallization. At 755 °C, on the plateau between the two exotherm peaks, NZP peaks and very low intensity ZrP_2O_7 peaks are detected while the most intense ZrO_2 peak is still present. At 850 °C, the ZrP_2O_7 peaks are sharp and well defined, indicating that the second exotherm is at least in part the result of ZrP_2O_7 formation. These data indicate initial NZP formation occurs at a lower temperature than ZrP_2O_7 formation, and that the two phases form in two distinct exothermic events. No thermal event was evident at higher temperatures, which would indicate the consumption of ZrP_2O_7, ZrO_2 and sodium compounds and the formation of NZP. This would be required for phase-pure NZP synthesis by this technique.

To determine whether phase-pure NZP monoliths, free of ZrP_2O_7 and ZrO_2, could be made by the *alkali nitrate method*, samples were heated for 24 h at 840, 940 and 1040 °C, and X-ray analysis carried out to determine which phases were present. At 840 and 940 °C, both NZP and ZrP_2O_7 were detected, but not ZrO_2. Phase-pure NZP was attained after heating for 24 h at 1040 °C. Therefore, the kinetics of the reaction consuming ZrP_2O_7 and ZrO_2 must be sufficiently slow that conversion cannot be observed by DTA to 1050 °C. Thus, although the *alkali nitrate* method produced castable NZP monoliths, the homogeneity of the reactants was low, making phase-pure material formation dependent upon diffusional processes similar to those required by solid-state synthesis techniques. As a result, the temperature required to achieve phase purity was high.

3.2. *Condensed alkali phosphate method*

A second technique, *the condensed alkali phosphate method*, was developed to improve homogeneity and lower temperature synthesis by elimination of the sodium nitrate reactant particles. The sodium was incorporated into the condensed phosphate by partially substituting for protons in polyphosphoric acid. As is the case for condensed phosphoric acid solutions, amorphous sodium acid phosphate containing equimolar amounts of Na_2O and H_2O ($H_2O/Na_2O = 1$) are composed of phosphate chains of varied lengths. In these sodium phosphates, the composite Na ion behaves similarly to protons in condensed phosphoric acid [10]. It was assumed that the condensed sodium phosphate solution used in this study, with $H_2O/Na_2O = 6.5$, was also comprised of phosphate chains, and that the distribution was similar to that observed in condensed phosphoric acid.

Fig. 5 shows the X-ray diffraction patterns of the products obtained at room temperature by reaction between zirconyl nitrate hydrate and condensed sodium phosphate after curing for one and 40 days. The presence of crystalline sodium nitrate indicates the synthesis modification had not eliminated it from these materials. Zirconium hydrogen phosphate hydrate (α-ZrP), an ion exchange phase with chemical formula $Zr(HPO_4)_2 \cdot H_2O$, was also present in these samples. The diffraction pattern of the sample cured for one day (excluding the $NaNO_3$ peak) is similar to that of a poorly crystalline sample prepared by hot precipitation [11], except for the noticeable absence of the $Zr(HPO_4)_2 \cdot H_2O$ (0 0 2) reflection at approximately 11°2θ. In the sample cured for 40 days, this (0 0 2) reflection was present; however, it had shifted to slightly lower 2θ (larger d-spacing) than that indicated by the JCPDS file for highly crystalline material. This result is in agreement with observations of Clearfield and Stynes [11], who synthesized completely amorphous

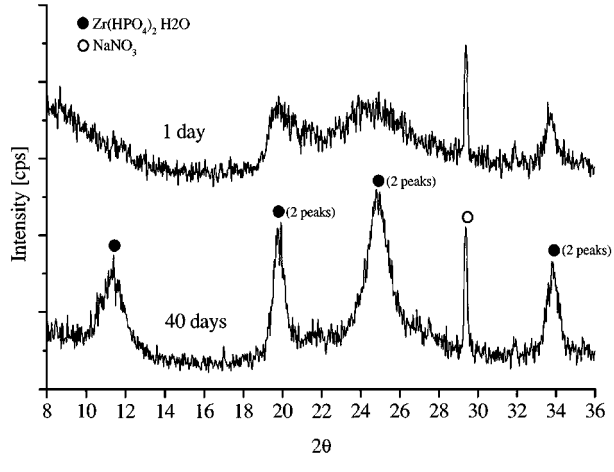

Figure 5 X-ray diffraction pattern of NZP precursor material prepared by the *condensed alkali phosphate method* after curing for one and 40 days at room temperature.

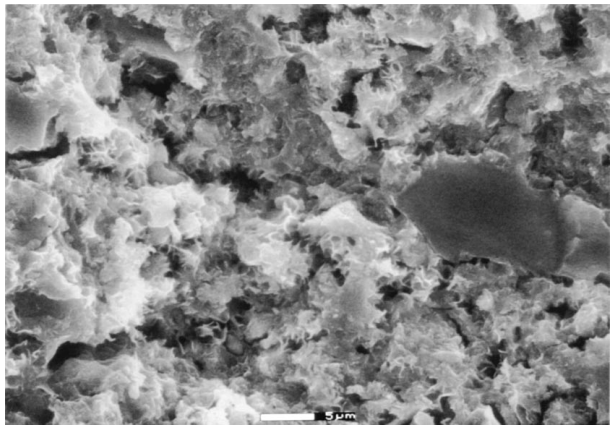

Figure 6 Micrograph of NZP precursor material prepared by the *condensed alkali phosphate method* and cured at room temperature.

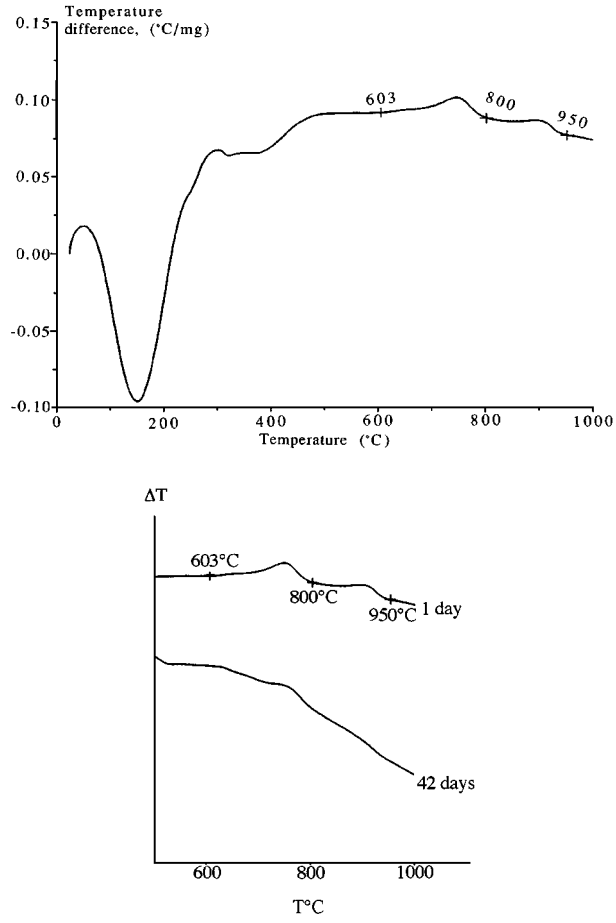

Figure 7 DTA curve obtained when NZP precursor materials prepared by the *condensed alkali phosphate method* are heated from 500 to 1000 °C.

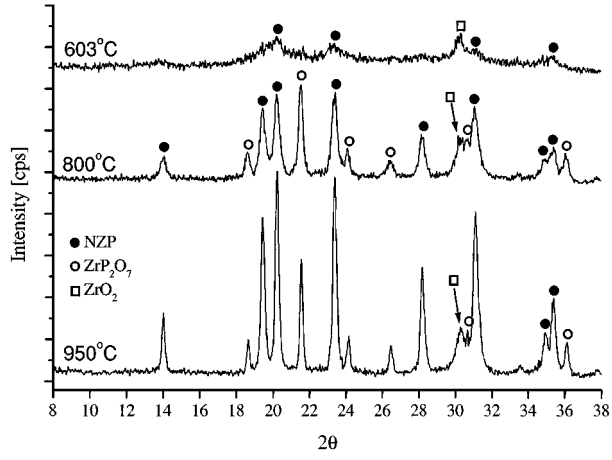

Figure 8 X-ray diffraction patterns obtained after precursor material prepared by *condensed alkali phosphate method* has been heated to 603, 800 and 950 °C.

to highly crystalline α-ZrP, and observed that poorly crystalline α-ZrP had larger d-spacings than the highly crystalline material. This shift was attributed to distortions in the crystal lattice. The increase in the intensities of the zirconium hydrogen phosphate hydrate peaks indicates that the α-ZrP becomes more crystalline with curing at room temperature.

Fig. 6 is a micrograph of a fracture surface of the room temperature reaction product. The microstructure is characterized by reactant particle artifacts covered by a reticulated structure. Distinct regions of localized concentrations of sodium attributed to the presence of sodium nitrate reactant particle artifacts in the *alkali-nitrate-method*-derived sample were not evident, indicating that homogeneity has been improved by this process modification.

Fig. 7 shows DTA plots for monoliths made by the *condensed alkali phosphate method* after curing for one and 42 days at room temperature. Crystallization exotherms similar to those in the DTA pattern for *alkali-nitrate-method*-derived monoliths appear in the DTA pattern of the sample cured for one day. Onset temperatures of approximately 570 and 860 °C can be observed. Crystallization exotherms are not nearly as well defined in the sample cured for 42 days. One distinct exotherm with onset temperature of approximately 710 °C is present. This suggests the phase formation is dependent upon the crystallinity of the α-ZrP present before heat treatment.

The same technique used to determine events responsible for exotherms in the DTA curve for the *alkali-nitrate-method*-derived material was used in the analysis of a sample made by the *condensed alkali phosphate method*, and cured for one day. The temperatures to which specimens were heated before X-ray diffraction data were collected are labelled in Fig. 7, and the X-ray patterns are shown in Fig. 8. X-ray results show that heating to 603 °C, the onset of the first exothermic event, results in the formation of poorly crystalline NZP and ZrO_2. After heating to 800 °C, a temperature above that of the first exotherm, the material contains NZP, ZrO_2 and ZrP_2O_7, indicating the exotherm to be the result of NZP, ZrO_2 and ZrP_2O_7 crystallization. After heating to 950 °C, these same three phases are present; however, the NZP peaks are of higher intensity, suggesting the second endotherm is the result of further NZP crystallization. These data indicate that unlike material prepared by the *alkali nitrate method*, the first exothermic event results in formation of both NZP and ZrP_2O_7, when the *condensed alkali phosphate method* is used. However, there is a considerable temperature range over which this thermal event occurs; this may be a result of two distinct crystallization events. The shape of the DTA peak, which rises gradually initially up to approximately 690 °C before forming a well defined

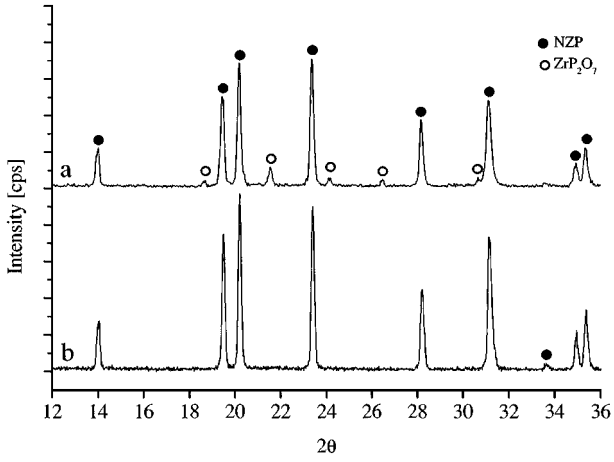

Figure 9 X-ray diffraction patterns obtained after precursor made by the two methods were heat treated at 940 °C for 24 h.

peak, is consistent with this. The X-ray data indicates that NZP formation initiates at lower temperature, as both NZP and ZrO_2 peaks are present in the pattern obtained after heating to 613 °C. Formation of ZrP_2O_7 appears to be responsible for the well defined DTA peak above 690 °C. The exotherms responsible for formation of NZP and ZrP_2O_7 are much more clearly resolved in the monoliths prepared by the *alkali nitrate method*, where these events are clearly resolved into two distinct peaks.

A monolith prepared by the *condensed alkali phosphate method* was heated for 24 h at 940 °C to determine if phase-pure NZP could be made by this technique. Fig. 9 compares the X-ray patterns for the *alkali-nitrate-method-* and *condensed-alkali-phosphate-method*-derived materials after heating at 940 °C. The *condensed-alkali-phosphate-method*-derived material has converted to phase-pure NZP, while the *alkali-nitrate-method*-derived material contains ZrP_2O_7. This difference is attributable to improved homogeneity of the *condensed-alkali-phosphate-method*-derived materials, by elimination of sodium nitrate reactant particle artifacts. Thus, the second exotherm in the DTA pattern for the *condensed alkali phosphate* material may be associated with the consumption of ZrP_2O_7 and ZrO_2 and formation of NZP, as the onset for this event is below 940 °C. If this is the case, the absence of a comparable thermal event in material made by the *alkali nitrate method* is consistent with the difficulty in achieving phase purity at 940 °C.

Acknowledgements

The authors acknowledge the support of the Cooperative Program in High Temperature Engineering Materials, Center for Advanced Materials at Pennsylvania State University. PWB also acknowledges the financial support of a National Science Foundation Grant DMR-9510272.

References

1. L. HAGMAN and P. KIERKEGAARD, *Acta Chem. Scand.* **22** (1968) 1822.
2. H. Y-P. HONG, *Mater. Res. Bull.* **11** (1976) 173.
3. J. B. GOODENOUGH, H. Y-P. HONG and J. A. KAFALAS, *Ibid.* **11** (1976) 203.
4. J. P. BOILOT, J. P. SALANIÉ, G. DESPLANCHES and D. L. POTIER, *Ibid.* **14** (1979) 1469.
5. J. ALAMO and R. ROY, *J. Amer. Ceram. Soc.* **67** (1984) C78.
6. R. ROY, D. K. AGRAWAL, J. ALAMO and R. A. ROY, *Mater. Res. Bull.* **19** (1984) 471.
7. J. ALAMO and R. ROY, *J. Mater. Sci.* **21** (1986) 444.
8. R. ROY, D. K. AGRAWAL and R. A. ROY, U.S. Patent 4 675 302, June (1987).
9. S. KOMERNENI, *Int. J. High Tech. Ceram.* **4** (1988) 31.
10. J. Van WAZER, "Phosphorous and its Compounds" (1958) p. 747.
11. A. CLEARFIELD and J. A. STYNES, *J. Inorg. Nuc. Chem.* **26** (1964) 117.
12. A. CLEARFIELD, L. KULBERG and Å. OSKARSSON, *J. Phys. Chem.* **73** (1969) 3424.

Received 27 October 1997
and accepted 24 June 1998